On extending and comparing Newton-Raphson variants for solving Power-Flow Equations

Simone Dutto, Giulio Masetti, *Student member, IEEE,* Silvano Chiaradonna,
Felicita Di Giandomenico, *Member, IEEE*

***Abstract*—This paper focuses on Power-Flow Equations solutions, based on the Newton-Raphson method. Two major contributions are offered. First, the definition of novel solution variants, resorting to Wirtinger calculus, is attempted. The obtained developments, although original in their formulation, led to already known variants. Despite the impaired originality of the obtained solution, there are significant lessons learned from such an effort. The second major contribution consists in a deep comparison analysis of existing solution strategies, based on complex and real variables, and the Wirtinger based ones, all properly reformulated to allow direct comparison with each other. The goal is to investigate strengths and weaknesses of the addressed techniques in terms of computational effort and convergence rate, which are the most relevant aspects to consider when making the choice of the approach to employ to solve power-flow equations for a specific power system under study.**

***Index Terms*—Newton-Raphson method, Jacobian matrices, load-flow analysis, sparse matrices, non-linear equation.**

I. Introduction

SOLVING the Power-Flow Equations (PFEs) is probably the most fundamental challenge posed by power systems analysis. In the literature, several solving methods have been adopted to tackle their solutions (e.g. [1], [2]). In particular, since the PFEs determine a large system of non-linear equations, iterative solving methods are preferred and this paper focuses on the Newton-Raphson method (NR) [3], that is one of the most used thanks to its robustness and its quadratic convergence. However, in order to use NR, the equations must be differentiable and, since the PFEs are non-holomorphic, different formulations are required. The process including formulation and solving method here is called *strategy*.

PFEs can be formulated using real or complex variables. After introducing the context in Section II, an overview of existing NR-based strategies and a brief discussion on their strengths and weaknesses are presented in Section III.

Since Wirtinger calculus can be directly applied to the complex formulation of the PFEs, Section IV investigates the adoption of the Wirtinger Jacobian in NR steps. After obtaining a complex-based strategy ($\text{NR}^{\text{W}\mathbb{C}}$), the structure of the Wirtinger Jacobian is exploited to get two real-based strategies ($\text{NR}^{\text{W}\mathbb{R}}$ and $\text{NR}^{\text{W}\mathbb{R}}_{red}$). Although their original formulation, $\text{NR}^{\text{W}\mathbb{C}}$ and $\text{NR}^{\text{W}\mathbb{R}}$ led to already known NR-based strategies.

Despite the originality is impaired, there is value in the performed exploration. The conducted study shed light on a direction that has an apparent promising starting point. In addition, the original formulations have an impact on the performance of the obtained strategies different from the existing counterparts.

Another major contribution of the paper is a deep comparison analysis among existing solution strategies, based on complex and real variables, and Wirtinger based ones, all properly reformulated to allow direct comparison with each other. Strengths and weaknesses of the addressed techniques are analyzed in Section V, in terms of computational effort and convergence rate. The results of this study can be usefully exploited by practitioners in making the best choice of the approach to employ to solve the PFEs for their specific system.

II. Context

The PFEs derive formally from the Ohm's law, the Kirchhoff's current law and the formula for the complex power (S) [1]. The common complex formulation of the resulting equation associated to a node *i* is given by:

$$\Delta S_i = E_i \overline{I_i^{\text{bus}}} - S_i = E_i \sum_{k \simeq i} \overline{Y_{ik}^{\text{bus}}}\,\overline{E}_k - S_i = 0 \qquad (1)$$

where E is the complex voltage, I^{bus} is the bus current, Y^{bus} is the bus admittance and $\simeq$ means *connected or equal to*. A variable is overlined when its *complex conjugate* is considered.

Equation (1) can be seen as a row of the matrix equation:

$$\Delta \mathbf{S} = [\mathbf{E}]\overline{\mathbf{Y}^{\text{bus}}}\,\overline{\mathbf{E}} - \mathbf{S} = \mathbf{0} \qquad (2)$$

where $\overline{\mathbf{E}}$ and $\mathbf{S}$ are vectors, $\mathbf{Y}^{\text{bus}}$ is a sparse matrix and $[\mathbf{E}]$ is the square matrix with the entries of the vector $\mathbf{E}$ on its diagonal and all zeros elsewhere.

In order to classify the buses nature, the complex power S and the complex voltage E are written using the *cartesian* and the *polar* coordinates respectively:

$$\begin{aligned} S &= \Re(S) + \jmath\Im(S) = P + \jmath Q \\ E &= |E|e^{\jmath\varphi(E)} = Ve^{\jmath\delta} = V(\cos(\delta) + \jmath\sin(\delta)) \end{aligned} \qquad (3)$$

where P and Q are real quantities called *active* and *reactive* power, while *magnitude* and *phase* of E are indicated with V and δ respectively. Given these coordinates, each bus of an electrical grid can be classified depending on which of the four real quantities just introduced are constant:

- there is always a single $V\delta$-bus, that has V and δ constant, called *slack* bus;
- PQ-buses have P and Q constant;
- PV-buses have P and V constant.

Then, the number of buses in a grid is $1 + N_{PQ} + N_{PV} = N$.

In the following matrix equations, the subscripts PQ, PV and $V\delta$ indicate the selection of rows corresponding to PQ-buses, PV-buses and $V\delta$-bus respectively.

The unknown values in the PFEs depend on the bus type associated to the index i: if i refers to the $V\delta$-bus, its complex power S has to be determined; if i is the index of a PQ-bus, then its voltage E is a complex unknown; if i is a PV-bus, the unknowns are Q and δ. Hence, the system (2) contains N complex equations in $1+N_{PQ}$ complex and $2N_{PV}$ real unknowns. Since $\mathbb{C}^{1+N_{PQ}} \times \mathbb{R}^{2N_{PV}}$ and $\mathbb{C}^N$ have the same dimension as vector spaces over $\mathbb{R}$, the number of equations in (2) is equal to its degree of freedom and, since the equations are linearly independent, the system is *consistent* (i.e., admits at least one solution). It is important to observe that the unknowns related to PV-buses can only be described with their real form, so that complex formulations of the equations are disadvantaged.

Solutions of a non-linear system of complex or real equations with lots of unknowns are not easy to be found with a direct method. Hence, the most straightforward way to solve systems like (2) is using an iterative method. One of the most used is the Newton-Raphson method (NR) [3]: starting from an initial approximation of the solution $\mathbf{X}^0$ of a system of equations $\mathbf{F}(\mathbf{X})=\mathbf{0}$, the corrections $\Delta\mathbf{X}^k = \mathbf{X}^{k+1}-\mathbf{X}^k$ are obtained by solving the linear equation system

$$\mathbf{J}(\mathbf{X}^k)\Delta\mathbf{X}^k = -\mathbf{F}(\mathbf{X}^k) \tag{4}$$

where $\mathbf{J} = (\partial F_i/\partial X_j)$ is the Jacobian matrix of $\mathbf{F}$. The iterative process is stopped when $|\mathbf{F}(\mathbf{X}^k)|_\infty < tol$.

Note that, when formulating the PFEs with complex variables, NR is not directly usable because of the complex conjugate $\overline{I_i^{\text{bus}}}$ in (1) that makes the equations non-holomorphic with respect to the complex variables E_i.

III. State of the art

In order to make NR exploitable in the PFEs context, most of the strategies formulate the complex system (2) with real variables and then construct $\mathbf{J}$ using the real derivatives (Section III-A). Other strategies, instead, maintain a complex formulation but calculate $\mathbf{J}$ with different derivatives (Sections III-B and IV).

In both cases, NR is particularly powerful in solving the PFEs because $\mathbf{J}$ maintains the sparsity of $\mathbf{Y}^{\text{bus}}$.

A. Real-based strategies

Depending on the real coordinates used for the voltages, there are two main real-based strategies.

1) Polar Coordinates [4]: when writing voltages with their polar coordinates, equation (1) becomes:

$$\Delta S_i = E_i e^{\jmath\delta_i}\sum_{k\simeq i}\overline{Y_{ik}^{\text{bus}}}V_k e^{-\jmath\delta_k} - S_i = 0 \tag{5}$$

and a real equation system can be obtained by considering $\Re(\Delta\mathbf{S}) = \Delta\mathbf{P}$ and $\Im(\Delta\mathbf{S}) = \Delta\mathbf{Q}$. In this case, the subsystem

$$\begin{cases} \Delta\mathbf{P}_{PQ} = \Re\Big([\mathbf{E}_{PQ}]\overline{\mathbf{Y}_{PQ}^{\text{bus}}}\overline{\mathbf{E}}\Big) - \mathbf{P}_{PQ} = \mathbf{0} \\ \Delta\mathbf{P}_{PV} = \Re\Big([\mathbf{E}_{PV}]\overline{\mathbf{Y}_{PV}^{\text{bus}}}\overline{\mathbf{E}}\Big) - \mathbf{P}_{PV} = \mathbf{0} \\ \Delta\mathbf{Q}_{PQ} = \Im\Big([\mathbf{E}_{PQ}]\overline{\mathbf{Y}_{PQ}^{\text{bus}}}\overline{\mathbf{E}}\Big) - \mathbf{Q}_{PQ} = \mathbf{0} \end{cases} \tag{6}$$

contains $2N_{PQ}+N_{PV}$ real equations in $2N_{PQ}+N_{PV}$ real unknowns and determines $\mathbf{F}(\boldsymbol{\delta}_{PQ,\,PV}, \mathbf{V}_{PQ}) = \mathbf{0}$ to be solved with NR. Its solutions, once found, can be replaced in the other subsystem containing the equations $\Delta\mathbf{P}_{V\delta} = \mathbf{0}$ and $\Delta\mathbf{Q}_{PV,V\delta} = \mathbf{0}$ to easily calculate all the remaining real unknowns $(\mathbf{P}_{V\delta}, \mathbf{Q}_{PV,\,V\delta})$. Since the derivatives of (6) can be calculated as the real and imaginary parts of:

$$\begin{aligned} \frac{\partial\Delta\mathbf{S}}{\partial\mathbf{V}} &= [\mathbf{E}]\Big([\overline{\mathbf{Y}^{\text{bus}}}\overline{\mathbf{E}}] + \overline{\mathbf{Y}^{\text{bus}}}[\overline{\mathbf{E}}]\Big)[\mathbf{V}^{-1}] \\ \frac{\partial\Delta\mathbf{S}}{\partial\boldsymbol{\delta}} &= \jmath[\mathbf{E}]\Big([\overline{\mathbf{Y}^{\text{bus}}}\overline{\mathbf{E}}] - \overline{\mathbf{Y}^{\text{bus}}}[\overline{\mathbf{E}}]\Big) \end{aligned} \tag{7}$$

the real Jacobian of $\mathbf{F}$ for (4) is given by:

$$\mathbf{J} = \left(\begin{array}{c|c} \mathbf{J}_{11} & \mathbf{J}_{12} \\ \hline \mathbf{J}_{21} & \mathbf{J}_{22} \end{array}\right) \in \mathbb{R}^{2N_{PQ}+N_{PV},\,2N_{PQ}+N_{PV}} \tag{8}$$

where:

$$\begin{aligned} \mathbf{J}_{11} &= \Re\left(\frac{\partial\Delta\mathbf{S}_{PQ,PV}}{\partial\boldsymbol{\delta}_{PQ,PV}}\right) & \mathbf{J}_{12} &= \Re\left(\frac{\partial\Delta\mathbf{S}_{PQ,PV}}{\partial\mathbf{V}_{PQ}}\right) \\ \mathbf{J}_{21} &= \Im\left(\frac{\partial\Delta\mathbf{S}_{PQ}}{\partial\boldsymbol{\delta}_{PQ,PV}}\right) & \mathbf{J}_{22} &= \Im\left(\frac{\partial\Delta\mathbf{S}_{PQ}}{\partial\mathbf{V}_{PQ}}\right) \end{aligned} \tag{9}$$

The strategy, consisting in solving the formulation (6) with NR through the Jacobian (8), is here indicated with NR^{PC}.

2) Rectangular Coordinates [3]: if the voltages are written with their rectangular coordinates, then equation (1) becomes:

$$\Delta S_i = (E_i^x + \jmath E_i^y)\sum_{k\simeq i}\overline{Y_{ik}^{\text{bus}}}(E_j^x - \jmath E_j^y) - S_i = 0 \tag{10}$$

As in the previous formulation, the subsystem containing the equations $\Delta\mathbf{P}_{V\delta}=\mathbf{0}$ and $\Delta\mathbf{Q}_{PV,V\delta}=\mathbf{0}$ can be easily solved after obtaining the voltages of PQ-buses and PV-buses. However, the system (6) contains only $2N_{PQ}+N_{PV}$ equations while the real unknowns $(\mathbf{E}_{PQ,PV}^x, \mathbf{E}_{PQ,PV}^y)$ are $2(N_{PQ}+N_{PV})$. Consequently, $\mathbf{F}(\mathbf{E}_{PQ,PV}^x, \mathbf{E}_{PQ,PV}^y) = \mathbf{0}$ has to be:

$$\begin{cases} \Delta\mathbf{P}_{PQ} = \Re\Big([\mathbf{E}_{PQ}]\overline{\mathbf{Y}_{PQ}^{\text{bus}}}\overline{\mathbf{E}}\Big) - \mathbf{P}_{PQ} = \mathbf{0} \\ \Delta\mathbf{P}_{PV} = \Re\Big([\mathbf{E}_{PV}]\overline{\mathbf{Y}_{PV}^{\text{bus}}}\overline{\mathbf{E}}\Big) - \mathbf{P}_{PV} = \mathbf{0} \\ \Delta\mathbf{Q}_{PQ} = \Im\Big([\mathbf{E}_{PQ}]\overline{\mathbf{Y}_{PQ}^{\text{bus}}}\overline{\mathbf{E}}\Big) - \mathbf{Q}_{PQ} = \mathbf{0} \\ \Delta\mathbf{V}_{PV}^2 = |\mathbf{E}_{PV}|^2 - \mathbf{V}_{PV}^2 = \mathbf{0} \end{cases} \tag{11}$$

so that there are $2(N_{PQ}+N_{PV}) = 2N-2$ equations and the PV-buses voltages respect the magnitude constraint.

Derivatives of (11) are given by:

$$\begin{aligned} \frac{\partial\Delta\mathbf{P}}{\partial\mathbf{E}^x} &= [\mathbf{G}^{\text{bus}}\mathbf{E}^x - \mathbf{B}^{\text{bus}}\mathbf{E}^y] + [\mathbf{E}^x]\mathbf{G}^{\text{bus}} + [\mathbf{E}^y]\mathbf{B}^{\text{bus}} \\ \frac{\partial\Delta\mathbf{P}}{\partial\mathbf{E}^y} &= [\mathbf{G}^{\text{bus}}\mathbf{E}^y + \mathbf{B}^{\text{bus}}\mathbf{E}^x] + [\mathbf{E}^y]\mathbf{G}^{\text{bus}} - [\mathbf{E}^x]\mathbf{B}^{\text{bus}} \\ \frac{\partial\Delta\mathbf{Q}}{\partial\mathbf{E}^x} &= -[\mathbf{G}^{\text{bus}}\mathbf{E}^y + \mathbf{B}^{\text{bus}}\mathbf{E}^x] + [\mathbf{E}^y]\mathbf{G}^{\text{bus}} - [\mathbf{E}^x]\mathbf{B}^{\text{bus}} \\ \frac{\partial\Delta\mathbf{Q}}{\partial\mathbf{E}^y} &= [\mathbf{G}^{\text{bus}}\mathbf{E}^x - \mathbf{B}^{\text{bus}}\mathbf{E}^y] - [\mathbf{E}^x]\mathbf{G}^{\text{bus}} - [\mathbf{E}^y]\mathbf{B}^{\text{bus}} \\ \frac{\partial\Delta\mathbf{V}^2}{\partial\mathbf{E}^x} &= [2\mathbf{E}^x] & \frac{\partial\Delta\mathbf{V}^2}{\partial\mathbf{E}^y} &= [2\mathbf{E}^y] \end{aligned} \tag{12}$$

where $\mathbf{G}^{\text{bus}} = \Re\big(\mathbf{Y}^{\text{bus}}\big)$ is the bus conductance matrix and $B^{\text{bus}} = \Im\big(\mathbf{Y}^{\text{bus}}\big)$ is the bus susceptance matrix.

Then, in (4) the Jacobian of $\mathbf{F}$ is:

$$\mathbf{J} = \left(\begin{array}{c|c} \mathbf{J}_{11} & \mathbf{J}_{12} \\ \hline \mathbf{J}_{21} & \mathbf{J}_{22} \\ \hline \mathbf{J}_{31} & \mathbf{J}_{32} \end{array}\right) \in \mathbb{R}^{2N-2,\,2N-2} \tag{13}$$

where:

$$\begin{aligned} \mathbf{J}_{11} &= \frac{\partial \Delta \mathbf{P}_{PQ,PV}}{\partial \mathbf{E}^{x}_{PQ,PV}} & \mathbf{J}_{12} &= \frac{\partial \Delta \mathbf{P}_{PQ,PV}}{\partial \mathbf{E}^{y}_{PQ,PV}} \\ \mathbf{J}_{21} &= \frac{\partial \Delta \mathbf{Q}_{PQ}}{\partial \mathbf{E}^{x}_{PQ,PV}} & \mathbf{J}_{22} &= \frac{\partial \Delta \mathbf{Q}_{PQ}}{\partial \mathbf{E}^{y}_{PQ,PV}} \\ \mathbf{J}_{31} &= \frac{\partial \Delta \mathbf{V}^{2}_{PV}}{\partial \mathbf{E}^{x}_{PQ,PV}} & \mathbf{J}_{32} &= \frac{\partial \Delta \mathbf{V}^{2}_{PV}}{\partial \mathbf{E}^{y}_{PQ,PV}} \end{aligned} \tag{14}$$

Solving (11) with NR and (13) as Jacobian determines a strategy here called $\mathrm{NR}^{\mathrm{RC}}$.

B. Complex-based strategies

Despite the fact that the complex conjugate makes equations (1) non-holomorphic with respect to the voltages, and hence impossible to differentiate using the classic complex derivatives, there are particular processes that make complex PFEs solvable with NR without converting them to their real version. An example, concerning an approximation of the complex Jacobian with respect to $\overline{E}$, can be seen in [5].

Another possibility consists in considering E and $\overline{E}$ as independent variables and use complex derivatives [6]. Since $\overline{E}$ are independent of the E, they generally differ from the complex conjugates of E and, in order to emphasize this difference, $\overline{E}$ will be indicated with W.

In this case, equation (1) becomes:

$$\Delta S_i = E_i \sum_{k \simeq i} \overline{Y^{\mathrm{bus}}_{ik}} W_k - S_i = 0 \tag{15}$$

and it is holomorphic with respect to E and W.

As in Section III-A, $\mathbf{P}_{V\delta}$ and $\mathbf{Q}_{PV,\,V\delta}$ can be determined from voltages, so that the unknowns of the system are $\mathbf{E}_{PQ,\,PV}$ and $\mathbf{W}_{PQ,\,PV}$. Since $2(N_{PQ}+N_{PV})$ complex unknowns are involved, in order to have $2(N_{PQ}+N_{PV})$ linearly independent equations, [6] considers the complex formulation:

$$\begin{cases} \Delta \mathbf{S}_{PQ} = [\mathbf{E}_{PQ}]\overline{\mathbf{Y}^{\mathrm{bus}}_{PQ}}\mathbf{W} - \mathbf{S}_{PQ} = \mathbf{0} \\ \Delta 2\mathbf{P}_{PV} = [\mathbf{E}_{PV}]\overline{\mathbf{Y}^{\mathrm{bus}}_{PV}}\mathbf{W} + [\mathbf{W}_{PV}]\mathbf{Y}^{\mathrm{bus}}_{PV}\mathbf{E} - 2\mathbf{P}_{PV} = \mathbf{0} \\ \Delta \overline{\mathbf{S}}_{PQ} = [\mathbf{W}_{PQ}]\mathbf{Y}^{\mathrm{bus}}_{PQ}\mathbf{E} - \overline{\mathbf{S}}_{PQ} = \mathbf{0} \\ \Delta \mathbf{V}^{2}_{PV} = [\mathbf{E}_{PV}]\mathbf{W}_{PV} - \mathbf{V}^{2}_{PV} = \mathbf{0} \end{cases} \tag{16}$$

In this case, complex derivatives are calculated as:

$$\begin{aligned} \frac{\partial \Delta \mathbf{S}}{\partial \mathbf{E}} &= [\overline{\mathbf{Y}^{\mathrm{bus}}}\mathbf{W}] & \frac{\partial \Delta \mathbf{S}}{\partial \mathbf{W}} &= [\mathbf{E}]\overline{\mathbf{Y}^{\mathrm{bus}}} \\ \frac{\partial \Delta 2\mathbf{P}}{\partial \mathbf{E}} &= [\mathbf{W}]\mathbf{Y}^{\mathrm{bus}} + [\overline{\mathbf{Y}^{\mathrm{bus}}}\mathbf{W}] & & \\ \frac{\partial \Delta 2\mathbf{P}}{\partial \mathbf{W}} &= [\mathbf{E}]\overline{\mathbf{Y}^{\mathrm{bus}}} + [\mathbf{Y}^{\mathrm{bus}}\mathbf{E}] & & \\ \frac{\partial \Delta \overline{\mathbf{S}}}{\partial \mathbf{E}} &= [\mathbf{W}]\mathbf{Y}^{\mathrm{bus}} & \frac{\partial \Delta \overline{\mathbf{S}}}{\partial \mathbf{W}} &= [\mathbf{Y}^{\mathrm{bus}}\mathbf{E}] \\ \frac{\partial \Delta \mathbf{V}^{2}}{\partial \mathbf{E}} &= [\mathbf{W}] & \frac{\partial \Delta \mathbf{V}^{2}}{\partial \mathbf{W}} &= [\mathbf{E}] \end{aligned} \tag{17}$$

Thus, in [6], (4) has $\mathbf{J}$ structured as follows:

$$\mathbf{J} = \left(\begin{array}{c|c} \mathbf{J}_{11} & \mathbf{J}_{12} \\ \hline \mathbf{J}_{21} & \mathbf{J}_{22} \\ \hline \mathbf{J}_{31} & \mathbf{J}_{32} \\ \hline \mathbf{J}_{41} & \mathbf{J}_{42} \end{array}\right) \in \mathbb{C}^{2N-2,\,2N-2} \tag{18}$$

where:

$$\begin{aligned} \mathbf{J}_{11} &= \frac{\partial \Delta \mathbf{S}_{PQ}}{\partial \mathbf{E}_{PQ,PV}} & \mathbf{J}_{12} &= \frac{\partial \Delta \mathbf{S}_{PQ}}{\partial \mathbf{W}_{PQ,PV}} \\ \mathbf{J}_{21} &= \frac{\partial \Delta 2\mathbf{P}_{PV}}{\partial \mathbf{E}_{PQ,PV}} & \mathbf{J}_{22} &= \frac{\partial \Delta 2\mathbf{P}_{PV}}{\partial \mathbf{W}_{PQ,PV}} \\ \mathbf{J}_{31} &= \frac{\partial \Delta \overline{\mathbf{S}}_{PQ}}{\partial \mathbf{E}_{PQ,PV}} & \mathbf{J}_{32} &= \frac{\partial \Delta \overline{\mathbf{S}}_{PQ}}{\partial \mathbf{W}_{PQ,PV}} \\ \mathbf{J}_{41} &= \frac{\partial \Delta \mathbf{V}^{2}_{PV}}{\partial \mathbf{E}_{PQ,PV}} & \mathbf{J}_{42} &= \frac{\partial \Delta \mathbf{V}^{2}_{PV}}{\partial \mathbf{W}_{PQ,PV}} \end{aligned} \tag{19}$$

The strategy introduced in [6], that aims to solve (16) by using (18) in a complex version of NR, here is called $\mathrm{NR}^{\mathrm{NV}}$.

C. Discussion

In $\mathrm{NR}^{\mathrm{PC}}$, trigonometric functions are required and their evaluations imply numerical approximations [7] that can affect the results when very high precision is required (although this is not the normal circumstance). For $\mathrm{NR}^{\mathrm{RC}}$, the equations in (11) are polynomials so that trigonometric functions are avoided. A comparison between $\mathrm{NR}^{\mathrm{PC}}$ and $\mathrm{NR}^{\mathrm{RC}}$ with and without optimal multipliers is presented in [8]. Another study on different load-flow methods based on polar or rectangular coordinates is conducted in [9].

Concerning $\mathrm{NR}^{\mathrm{NV}}$, it allows to model particular devices, as reported in [6], but all computational costs are increased because of the complex calculus. In addition, since E and W are treated as independent variables, $\overline{E}$ and W can differ during $\mathrm{NR}^{\mathrm{NV}}$ steps, resulting in less accurate outcomes.

Moving from the above considerations and aiming at improving on the reported weaknesses, new formulations are investigated, resorting to the Wirtinger calculus because it is directly applicable to the complex formulation of the PFEs.

IV. Exploring Wirtinger calculus

The *Wirtinger derivatives* [10] exploit the fact that each complex function $\mathbf{F} : \mathbb{C}^m \to \mathbb{C}^m$ can be seen as $\tilde{\mathbf{F}} : \mathbb{R}^{2m} \to \mathbb{C}^m$ by writing its complex variables as $Z_i = X_i + \jmath Y_i$.

Hence, if $\tilde{\mathbf{F}}$ is differentiable in the real variables X_i and Y_i, the Wirtinger derivatives of $\mathbf{F}$ are defined as the following partial differential operators:

$$\frac{\partial^{w}\mathbf{F}}{\partial Z_i} = \frac{1}{2}\left(\frac{\partial \tilde{\mathbf{F}}}{\partial X_i} - \jmath\frac{\partial \tilde{\mathbf{F}}}{\partial Y_i}\right) \quad \frac{\partial^{w}\mathbf{F}}{\partial \overline{Z}_i} = \frac{1}{2}\left(\frac{\partial \tilde{\mathbf{F}}}{\partial X_i} + \jmath\frac{\partial \tilde{\mathbf{F}}}{\partial Y_i}\right) \tag{20}$$

It is important to observe that Wirtinger derivatives can be calculated without introducing $\tilde{\mathbf{F}}$. In this case, $\partial^{w}\mathbf{F}/\partial Z_i$ works as the classic complex derivative $\partial \mathbf{F}/\partial Z_i$ in which $\overline{Z}_i$ is considered as a constant, and the behaviour of $\partial^{w}\mathbf{F}/\partial \overline{Z}_i$ is the same of $\partial \mathbf{F}/\partial \overline{Z}_i$ with Z_i constant.

This property makes Wirtinger derivatives defined also for complex functions that are non-holomorphic because of the complex conjugate.

As for the classic complex derivatives, also for Wirtinger derivatives a Jacobian can be considered. However, since the matrix containing all Wirtinger derivatives of $\mathbf{F}$ is not square, the *Wirtinger Jacobian* is defined as:

$$\mathbf{J}^W = \left(\begin{array}{c|c} \frac{\partial^W \mathbf{F}}{\partial \mathbf{Z}} & \frac{\partial^W \mathbf{F}}{\partial \overline{\mathbf{Z}}} \\ \hline \frac{\partial^W \overline{\mathbf{F}}}{\partial \mathbf{Z}} & \frac{\partial^W \overline{\mathbf{F}}}{\partial \overline{\mathbf{Z}}} \end{array}\right) = \left(\begin{array}{c|c} \frac{\partial^W \mathbf{F}}{\partial \mathbf{Z}} & \frac{\partial^W \mathbf{F}}{\partial \overline{\mathbf{Z}}} \\ \hline \overline{\frac{\partial^W \mathbf{F}}{\partial \overline{\mathbf{Z}}}} & \overline{\frac{\partial^W \mathbf{F}}{\partial \mathbf{Z}}} \end{array}\right) \tag{21}$$

If the complex system $\mathbf{F}(\mathbf{Z}) = \mathbf{0}$ has to be solved, the Wirtinger Jacobian of $\mathbf{F}$ can be used in NR. Thus, analogously to (4), the correction $\Delta\mathbf{Z}$ is obtained by solving:

$$\mathbf{J}^W \left(\begin{array}{c} \Delta\mathbf{Z} \\ \hline \overline{\Delta\mathbf{Z}} \end{array}\right) = - \left(\begin{array}{c} \mathbf{F}(\mathbf{Z}) \\ \hline \overline{\mathbf{F}(\mathbf{Z})} \end{array}\right) \tag{22}$$

Since the PFEs contain complex conjugates that make them non-holomorphic with respect to the complex voltages, Wirtinger calculus is very appropriate to differentiate them.

An approach similar to the proposed one was introduced in [11] to differentiate the PFEs with respect to the electric currents, but for the different purpose of finding a necessary condition for power-flow insolvability in systems with distributed generators. Another interesting similar approach was introduced in [12] where, after considering Wirtinger derivatives, a solving method using complex tableaux is presented.

In order to use Wirtinger calculus, the PFEs have to be formulated with an appropriate system of complex equations. The number of these equations must be $N_{PQ} + N_{PV}$, which is the number of the unknown complex voltages $\mathbf{E}_{PQ,\,PV}$ (as in Section III, $\mathbf{P}_{V\delta}$ and $\mathbf{Q}_{PV,\,V\delta}$ can be easily determined later).

The PFEs and the constraints given by the bus types must be respected. Thus the first N_{PQ} equations can be simply (1) while, for PV-buses, the following N_{PV} complex equations, introduced in [13], are considered:

$$\Delta F_i = 2\Re\left(E_i \sum_{k \simeq i} \overline{Y_{ik}^{\text{bus}}}\,\overline{E}_k\right) - 2P_i + \jmath(|E_i|^2 - V_i^2) = 0 \tag{23}$$

The complex system $\mathbf{F}(\mathbf{E}_{PQ,PV}) = \mathbf{0}$ is consequently given by:

$$\begin{cases} \Delta\mathbf{S}_{PQ} = [\mathbf{E}_{PQ}]\overline{\mathbf{Y}_{PQ}^{\text{bus}}}\,\overline{\mathbf{E}} - \mathbf{S}_{PQ} = \mathbf{0} \\ \Delta\mathbf{F}_{PV} = 2\Re\left([\mathbf{E}_{PV}]\overline{\mathbf{Y}_{PV}^{\text{bus}}}\,\overline{\mathbf{E}}\right) - 2\mathbf{P}_{PV} + \jmath(|\mathbf{E}_{PV}|^2 - \mathbf{V}_{PV}^2) = \mathbf{0} \end{cases} \tag{24}$$

Equations (23) imply that the active power and the voltage magnitude of each PV-bus respect the constraints and, in addition, $\mathbf{F}$ has a non-singular Wirtinger Jacobian. Other equations for PV-buses can be found, paying attention to obtain a non-singular Wirtinger Jacobian matrix.

The Wirtinger derivatives of $\mathbf{F}$ are:

$$\begin{aligned} \frac{\partial^W \Delta\mathbf{S}}{\partial \mathbf{E}} &= [\overline{\mathbf{Y}^{\text{bus}}}\,\overline{\mathbf{E}}] & \frac{\partial^W \Delta\mathbf{S}}{\partial \overline{\mathbf{E}}} &= [\mathbf{E}]\overline{\mathbf{Y}^{\text{bus}}} \\ \frac{\partial^W \Delta\mathbf{F}}{\partial \mathbf{E}} &= [\overline{\mathbf{E}}]\mathbf{Y}^{\text{bus}} + [\overline{\mathbf{Y}^{\text{bus}}}\,\overline{\mathbf{E}} + \jmath\overline{\mathbf{E}}] \\ \frac{\partial^W \Delta\mathbf{F}}{\partial \overline{\mathbf{E}}} &= [\mathbf{E}]\overline{\mathbf{Y}^{\text{bus}}} + [\mathbf{Y}^{\text{bus}}\mathbf{E} + \jmath\mathbf{E}] \end{aligned} \tag{25}$$

It is noteworthy that, although the system of equations in (24) and the derivatives in (25) have the same structure of those related to NR^{NV} in (16) and (17), the number of independent variables, and consequently of derivatives, is halved. In fact, while with NR^{NV} $\mathbf{W}$ is independent of $\mathbf{E}$ and hence $\mathbf{W}$ slightly differs from $\overline{\mathbf{E}}$, with Wirtinger derivatives $\overline{\mathbf{E}}$ is exactly the complex conjugate of $\mathbf{E}$.

The Wirtinger Jacobian of $\mathbf{F}$ can be structured with only four blocks, as observed in (21):

$$\mathbf{J}^W = \left(\begin{array}{c|c} \mathbf{J}_{11}^W & \mathbf{J}_{12}^W \\ \hline \mathbf{J}_{21}^W & \mathbf{J}_{22}^W \\ \hline \overline{\mathbf{J}_{12}^W} & \overline{\mathbf{J}_{11}^W} \\ \hline \overline{\mathbf{J}_{22}^W} & \overline{\mathbf{J}_{21}^W} \end{array}\right) = \left(\begin{array}{c|c} \mathbf{A} & \mathbf{B} \\ \hline \overline{\mathbf{B}} & \overline{\mathbf{A}} \end{array}\right) \tag{26}$$

where:

$$\begin{aligned} \mathbf{J}_{11}^W &= \frac{\partial^W \Delta\mathbf{S}_{PQ}}{\partial \mathbf{E}_{PQ,PV}} & \mathbf{J}_{12}^W &= \frac{\partial^W \Delta\mathbf{S}_{PQ}}{\partial \overline{\mathbf{E}}_{PQ,PV}} \\ \mathbf{J}_{21}^W &= \frac{\partial^W \Delta\mathbf{F}_{PV}}{\partial \mathbf{E}_{PQ,PV}} & \mathbf{J}_{22}^W &= \frac{\partial^W \Delta\mathbf{F}_{PV}}{\partial \overline{\mathbf{E}}_{PQ,PV}} \end{aligned} \tag{27}$$

Despite starting from a different formulation, the Wirtinger derivatives exploited to obtain the matrix (26) actually returns the same Jacobian obtained in [13] through differential forms.

The strategy that uses the Wirtinger Jacobian (26) in NR to solve (24), here is called $\text{NR}^{\text{W}\mathbb{C}}$.

An improvement of $\text{NR}^{\text{W}\mathbb{C}}$ can be obtained through a real conversion of $\mathbf{J}^W$, exploiting its particular structure as follows.

The new-found conversion starts with inverting the order of the last $n = N_{PQ} + N_{PV}$ rows and columns of $\mathbf{J}^W$, in order to obtain a *centrohermitian* matrix [14], defined as:

$$\mathbf{M} \in \mathbb{C}^{m,m} | M_{ij} = \overline{M}_{m+1-i,m+1-j}, \text{ for } 1 \le i,j \le m \tag{28}$$

The permutation of indices that allows the conversion of $\mathbf{J}^W$ into a centrohermitian matrix is $\pi : i \mapsto 3n + 1 - i$ for $n < i \le 2n$. The matrix form $\mathbf{P}_\pi$ of π contains the matrices:

$$\mathbb{I}_n = \begin{pmatrix} 1 & & 0 \\ & \ddots & \\ 0 & & 1 \end{pmatrix}, \quad \mathbb{J}_n = \begin{pmatrix} 0 & & 1 \\ & \iddots & \\ 1 & & 0 \end{pmatrix} \in \mathbb{R}^{n,\,n} \tag{29}$$

known as *identity* and *exchange* matrix respectively, so that:

$$\mathbf{P}_\pi = \left(\begin{array}{c|c} \mathbb{I}_n & \mathbf{0}_n \\ \hline \mathbf{0}_n & \mathbb{J}_n \end{array}\right) \tag{30}$$

The action of π on $\mathbf{J}^W$, using $\mathbf{P}_\pi$, determines:

$$\mathbf{P}_\pi \left(\begin{array}{c|c} \mathbf{A} & \mathbf{B} \\ \hline \overline{\mathbf{B}} & \overline{\mathbf{A}} \end{array}\right) \mathbf{P}_\pi = \left(\begin{array}{c|c} \mathbf{A} & \mathbf{B}\mathbb{J}_n \\ \hline \mathbb{J}_n\overline{\mathbf{B}} & \mathbb{J}_n\overline{\mathbf{A}}\mathbb{J}_n \end{array}\right) \tag{31}$$

that satisfies (28) and thus is a centrohermitian matrix.

In particular, using π as in (31), every Wirtinger Jacobian is similar to a centrohermitian matrix.

As demonstrated in [14], every centrohermitian matrix is similar to a real matrix. In fact, given the *unitary* (i.e., $\mathbf{U}^{-1} = \mathbf{U}^* = \overline{\mathbf{U}^t}$) matrix:

$$\mathbf{U} = \frac{1}{\sqrt{2}} \left(\begin{array}{c|c} \mathbb{I}_n & \jmath\mathbb{I}_n \\ \hline \mathbb{J}_n & -\jmath\mathbb{J}_n \end{array}\right) \in \mathbb{C}^{2n,\,2n} \tag{32}$$

the centrohermitian matrix determined in (31) is similar to the real matrix:

$$\begin{aligned}&\mathbf{U}^*\left(\begin{array}{c|c}\mathbf{A} & \mathbf{B}\mathbb{J}_N\\ \hline \mathbb{J}_N\overline{\mathbf{B}} & \mathbb{J}_N\overline{\mathbf{A}}\mathbb{J}_N\end{array}\right)\mathbf{U}\\ &=\left(\begin{array}{c|c}\Re(\mathbf{A}+\mathbf{B}) & \Im(\mathbf{B}-\mathbf{A})\\ \hline \Im(\mathbf{A}+\mathbf{B}) & \Re(\mathbf{A}-\mathbf{B})\end{array}\right)=\mathbf{J}^{W\mathbb{R}}\end{aligned} \tag{33}$$

The matrix transformations described in (31) and (33) influence the system (22) as follows. Starting from:

$$\mathbf{J}^{W}\left(\begin{array}{c}\Delta\mathbf{E}\\ \hline \Delta\overline{\mathbf{E}}\end{array}\right)=\left(\begin{array}{c|c}\mathbf{A} & \mathbf{B}\\ \hline \overline{\mathbf{B}} & \overline{\mathbf{A}}\end{array}\right)\left(\begin{array}{c}\Delta\mathbf{E}\\ \hline \Delta\overline{\mathbf{E}}\end{array}\right)=-\left(\begin{array}{c}\mathbf{F}\\ \hline \overline{\mathbf{F}}\end{array}\right) \tag{34}$$

where $\Delta\mathbf{E}=\Delta\mathbf{E}_{PQ,PV}$ and $\mathbf{F}=\mathbf{F}(\mathbf{E}_{PQ,PV})$ is the left-hand side of the system in (24), the result of the permutation introduced in (31) is:

$$\begin{aligned}&\mathbf{P}_\pi\left(\begin{array}{c|c}\mathbf{A} & \mathbf{B}\\ \hline \overline{\mathbf{B}} & \overline{\mathbf{A}}\end{array}\right)\mathbf{P}_\pi\mathbf{P}_\pi\left(\begin{array}{c}\Delta\mathbf{E}\\ \hline \Delta\overline{\mathbf{E}}\end{array}\right)=-\mathbf{P}_\pi\left(\begin{array}{c}\mathbf{F}\\ \hline \overline{\mathbf{F}}\end{array}\right)\\ &\left(\begin{array}{c|c}\mathbf{A} & \mathbf{B}\mathbb{J}_N\\ \hline \mathbb{J}_N\overline{\mathbf{B}} & \mathbb{J}_N\overline{\mathbf{A}}\mathbb{J}_N\end{array}\right)\left(\begin{array}{c}\Delta\mathbf{E}\\ \hline \mathbb{J}_N\overline{\Delta\mathbf{E}}\end{array}\right)=-\left(\begin{array}{c}\mathbf{F}\\ \hline \mathbb{J}_N\overline{\mathbf{F}}\end{array}\right)\end{aligned} \tag{35}$$

and, considering the similitude in (33), (35) becomes:

$$\begin{aligned}&\mathbf{U}^*\left(\begin{array}{c|c}\mathbf{A} & \mathbf{B}\mathbb{J}_N\\ \hline \mathbb{J}_N\overline{\mathbf{B}} & \mathbb{J}_N\overline{\mathbf{A}}\mathbb{J}_N\end{array}\right)\mathbf{U}\mathbf{U}^*\left(\begin{array}{c}\Delta\mathbf{E}\\ \hline \mathbb{J}_N\overline{\Delta\mathbf{E}}\end{array}\right)=-\mathbf{U}^*\left(\begin{array}{c}\mathbf{F}\\ \hline \mathbb{J}_N\overline{\mathbf{F}}\end{array}\right)\\ &\mathbf{J}^{W\mathbb{R}}\tfrac{1}{\sqrt{2}}\left(\begin{array}{c}\Delta\mathbf{E}+\overline{\Delta\mathbf{E}}\\ \hline \Delta\mathbf{E}-\overline{\Delta\mathbf{E}}\end{array}\right)=-\tfrac{1}{\sqrt{2}}\left(\begin{array}{c}\mathbf{F}+\overline{\mathbf{F}}\\ \hline \mathbf{F}-\overline{\mathbf{F}}\end{array}\right)\\ &\mathbf{J}^{W\mathbb{R}}\left(\begin{array}{c}\Re(\Delta\mathbf{E})\\ \hline \Im(\Delta\mathbf{E})\end{array}\right)=-\left(\begin{array}{c}\Re(\mathbf{F})\\ \hline \Im(\mathbf{F})\end{array}\right)\end{aligned} \tag{36}$$

so that the resulting system has size $2(N_{PQ}+N_{PV})$ and contains only real values. The obtained real implementation of $\mathrm{NR}^{\mathrm{W}\mathbb{C}}$ is called $\mathrm{NR}^{\mathrm{W}\mathbb{R}}$.

The determined linear equation system of $\mathrm{NR}^{\mathrm{W}\mathbb{R}}$, although obtained through novel developments, is the same as the one of $\mathrm{NR}^{\mathrm{RC}}$. However, despite the same outcome from both strategies, the comparison studies described in Section V show that the differences in the construction of the Jacobian have an impact on the overall performance of the strategies, with $\mathrm{NR}^{\mathrm{W}\mathbb{R}}$ performing better than the classical $\mathrm{NR}^{\mathrm{RC}}$.

The structure of $\mathbf{J}^{W\mathbb{R}}$ is exploitable to further reduce the number of equations in (36).

In particular, in (33) the last N_{PV} rows of $\mathbf{J}^{W\mathbb{R}}$ are:

$$\left(\begin{array}{c|c}\cdots & \cdots\\ \hline \Im(\mathbf{J}^W_{21}+\mathbf{J}^W_{22}) & \Re(\mathbf{J}^W_{21}-\mathbf{J}^W_{22})\end{array}\right) \tag{37}$$

where, from (25):

$$\begin{aligned}\frac{\partial^W\Delta\mathbf{F}}{\partial\mathbf{E}}+\frac{\partial^W\Delta\mathbf{F}}{\partial\overline{\mathbf{E}}}&=2\Re\Big([\overline{\mathbf{E}}]\mathbf{Y}^{\text{bus}}+[\overline{\mathbf{Y}^{\text{bus}}}\overline{\mathbf{E}}]\Big)\\ &\quad+\jmath 2\Re([\mathbf{E}])\\ \frac{\partial^W\Delta\mathbf{F}}{\partial\mathbf{E}}-\frac{\partial^W\Delta\mathbf{F}}{\partial\overline{\mathbf{E}}}&=2\Im([\mathbf{E}])\\ &\quad+\jmath 2\Im\Big([\overline{\mathbf{E}}]\mathbf{Y}^{\text{bus}}+[\overline{\mathbf{Y}^{\text{bus}}}\overline{\mathbf{E}}]\Big)\end{aligned} \tag{38}$$

so that, from (27):

$$\begin{aligned}\Im(\mathbf{J}^W_{21}+\mathbf{J}^W_{22})&=\Big(\mathbf{0}\;\Big|\;[\,2\Re(\mathbf{E}_{PV})\,]\Big)\in\mathbb{R}^{N_{PQ}+N_{PV},N_{PV}}\\ \Re(\mathbf{J}^W_{21}-\mathbf{J}^W_{22})&=\Big(\mathbf{0}\;\Big|\;[\,2\Im(\mathbf{E}_{PV})\,]\Big)\in\mathbb{R}^{N_{PQ}+N_{PV},N_{PV}}\end{aligned} \tag{39}$$

Hence, the system (36) can be written as:

$$\left(\begin{array}{c|c|c|c}\mathbf{J}_1 & \mathbf{J}_2 & \mathbf{J}_3 & \mathbf{J}_4\\ \hline \mathbf{0} & \mathbf{D}_1 & \mathbf{0} & \mathbf{D}_2\end{array}\right)\left(\begin{array}{c}\Re(\Delta\mathbf{E}_{PQ})\\ \Re(\Delta\mathbf{E}_{PV})\\ \Im(\Delta\mathbf{E}_{PQ})\\ \Im(\Delta\mathbf{E}_{PV})\end{array}\right)=-\left(\begin{array}{c}\Re(\,\mathbf{F}\,)\\ \\ \Im(\mathbf{F}_{PQ})\\ \Im(\mathbf{F}_{PV})\end{array}\right) \tag{40}$$

where $\mathbf{D}_1=[\,2\Re(\mathbf{E}_{PV})\,]$ and $\mathbf{D}_2=[\,2\Im(\mathbf{E}_{PV})\,]$ are diagonal matrices. Calling $\hat{\mathbf{F}}$ the vector containing $\Re(\,\mathbf{F}\,)$ and $\Im(\mathbf{F}_{PQ})$, the submatrices equations related to (40) are:

$$\begin{cases}\mathbf{J}_1\Re(\Delta\mathbf{E}_{PQ})+\mathbf{J}_2\Re(\Delta\mathbf{E}_{PV})\\ \qquad+\mathbf{J}_3\Im(\Delta\mathbf{E}_{PQ})+\mathbf{J}_4\Im(\Delta\mathbf{E}_{PV})=-\hat{\mathbf{F}}\\ \mathbf{D}_1\Re(\Delta\mathbf{E}_{PV})+\mathbf{D}_2\Im(\Delta\mathbf{E}_{PV})=-\Im(\mathbf{F}_{PV})\end{cases} \tag{41}$$

In the second equation of (41), the real diagonal matrix $\mathbf{D}_1$ is always invertible, so that $\Re(\Delta\mathbf{E}_{PV})$ can be isolated:

$$\Re(\Delta\mathbf{E}_{PV})=-\mathbf{D}_1^{-1}\big(\mathbf{D}_2\Im(\Delta\mathbf{E}_{PV})+\Im(\mathbf{F}_{PV})\big) \tag{42}$$

and then substituted in the first equation of (41):

$$\begin{aligned}&\mathbf{J}_1\Re(\Delta\mathbf{E}_{PQ})-\mathbf{J}_2\mathbf{D}_1^{-1}\big(\mathbf{D}_2\Im(\Delta\mathbf{E}_{PV})+\Im(\mathbf{F}_{PV})\big)\\ &\qquad+\mathbf{J}_3\Im(\Delta\mathbf{E}_{PQ})+\mathbf{J}_4\Re(\Delta\mathbf{E}_{PV})=-\hat{\mathbf{F}}\end{aligned} \tag{43}$$

In conclusion, only the following submatrices equation has to be solved with an iterative method:

$$\begin{aligned}&\mathbf{J}_1\Re(\Delta\mathbf{E}_{PQ})+\mathbf{J}_3\Im(\Delta\mathbf{E}_{PQ})\\ &+\big(\mathbf{J}_4-\mathbf{J}_2\mathbf{D}_1^{-1}\mathbf{D}_2\big)\Im(\Delta\mathbf{E}_{PV})=-\hat{\mathbf{F}}+\mathbf{J}_2\mathbf{D}_1^{-1}\Im(\mathbf{F}_{PV})\end{aligned} \tag{44}$$

that is a linear system of equations of size $2N_{PQ}+N_{PV}$. The square matrix associated to (44) is given by:

$$\mathbf{J}^{W\mathbb{R}}_{\text{red}}=\left(\begin{array}{c|c}\mathbf{J}_1 & \mathbf{J}_3\\ \hline & \mathbf{J}_4-\mathbf{J}_2\mathbf{D}_1^{-1}\mathbf{D}_2\end{array}\right) \tag{45}$$

and determines a real and reduced version of $\mathrm{NR}^{\mathrm{W}\mathbb{C}}$ that here is called $\mathrm{NR}^{\mathrm{W}\mathbb{R}}_{red}$.

V. Comparison results

This section is devoted to compare the six strategies $\mathrm{NR}^{\mathrm{PC}}$, $\mathrm{NR}^{\mathrm{RC}}$, $\mathrm{NR}^{\mathrm{NV}}$, $\mathrm{NR}^{\mathrm{W}\mathbb{C}}$, $\mathrm{NR}^{\mathrm{W}\mathbb{R}}$ and $\mathrm{NR}^{\mathrm{W}\mathbb{R}}_{red}$, in terms of two major indicators representative of the quality of a PFEs solution strategy: computational effort and convergence to a solution. Therefore, theoretical analysis and experimental results about the computational costs are presented in Section V-A, while convergence rates are discussed in Section V-B.

All the experimental results are obtained through MATLAB [15] implementations of the strategies. $\mathrm{NR}^{\mathrm{PC}}$ was already part of MATPOWER [4], a MATLAB package for solving power-flow and optimal power-flow problems, while the other

strategies have been implemented by the authors. The choice of MATLAB presents two major advantages: first, it is based on matrices manipulations so that the implementations directly reflect the mathematical descriptions presented in this article; second, MATPOWER functionalities can be fully exploited.

Eleven case studies, included in the MATPOWER package [16] and inspired by real electrical networks, are considered. In particular, some of the larger cases are selected, precisely case1354pegase, case1888rte, case2000tex, case2383wp, case2746wp, case2868rte, case2869pegase, case3375wp, case6470rte, case9241pegase and case13659pegase (the number in the name is the number of buses involved).

A. Computational analysis

The focus is on a single step of NR in each strategy. The analysis distinguishes between the two major parts composing a step: the matrices construction and the linear system solution.

In order to cover in more general terms the comparison study and provide a comprehensive analysis, the strategies are compared with: 1) a theoretical analysis of the computational burden for the matrices construction; 2) a count of the operations required in the linear system solver; 3) an assessment of the elapsed times in MATLAB.

1) Matrices Construction: the first theoretical comparison consists in counting the number of loads, stores, real additions and real multiplications required to calculate $\mathbf{F}$ and $\mathbf{J}$ for (4) in each strategy step. This is a technology independent analysis, since it does not make any assumption on the specific computer architecture adopted to execute the strategy.

The methodology selected is inspired by the work in [17]. Following the definitions of complex operators, complex sums count as to two real additions, complex multiplications as two real sums and four real products, while reading and writing a complex number consist respectively in loading and storing two real quantities.

The aforementioned quantities are determined in terms of:

- the number of buses N;
- the number of PQ-buses N_{PQ};
- the number of lines L;
- the number of lines connecting PQ-buses $L_{PQ,PQ}$;
- the number of lines from PQ-buses to PV-buses $L_{PQ,PV}$;
- the number of lines connecting PV-buses $L_{PV,PV}$.

The presence of $L_{PQ,PQ}$, $L_{PQ,PV}$ and $L_{PV,PV}$ is due to the sparsity of the involved matrices that is conditioned by the sparsity of Y^{bus}.

$\mathbf{F}$ *in NR*$^{\text{PC}}$ *steps* (6):

$$\begin{aligned} load&\ 15N-1+N_{PQ}+16L\\ store&\ 9N-1+N_{PQ}+8L\\ add.&\ 6N+8L\\ mult.&\ 10N+8L \end{aligned}$$

This evaluation involves also $2N$ trigonometric functions.

$\mathbf{J}$ *in NR*$^{\text{PC}}$ *steps* (8):

$$\begin{aligned} load&\ 20N-1+3N_{PQ}+30L+8L_{PQ,PQ}+4L_{PQ,PV}+2L_{PV,PV}\\ store&\ 11N-1+3N_{PQ}+16L+8L_{PQ,PQ}+4L_{PQ,PV}+2L_{PV,PV}\\ add.&\ 8N+12L\\ mult.&\ 10N+20L \end{aligned}$$

$\mathbf{F}$ *in NR*$^{\text{RC}}$ *steps* (11):

$$\begin{aligned} load&\ 19N-7-5N_{PQ}+16L\\ store&\ 11N-5-3N_{PQ}+8L\\ add.&\ 8N-2-2N_{PQ}+8L\\ mult.&\ 10N-2-2N_{PQ}+8L \end{aligned}$$

$\mathbf{J}$ *in NR*$^{\text{RC}}$ *steps* (13):

$$\begin{aligned} load&\ 30N-6+2N_{PQ}+40L+8L_{PQ,PQ}+8L_{PQ,PV}+4L_{PV,PV}\\ store&\ 16N-4+20L+8L_{PQ,PQ}+8L_{PQ,PV}+4L_{PV,PV}\\ add.&\ 6N-2+2N_{PQ}+12L\\ mult.&\ 8N+8L \end{aligned}$$

$\mathbf{F}$ *in NR*$^{\text{NV}}$ *steps* (16):

$$\begin{aligned} load&\ 35N-11-7N_{PQ}+32L\\ store&\ 18N-6-2N_{PQ}+16L\\ add.&\ 17N-5-5N_{PQ}+16L\\ mult.&\ 20N-4-4N_{PQ}+16L \end{aligned}$$

$\mathbf{J}$ *in NR*$^{\text{NV}}$ *steps* (18):

$$\begin{aligned} load&\ 28N-12-4N_{PQ}+48L+8L_{PQ,PQ}+8L_{PQ,PV}+8L_{PV,PV}\\ store&\ 16N-8+24L+8L_{PQ,PQ}+8L_{PQ,PV}+8L_{PV,PV}\\ add.&\ 12N-4-4N_{PQ}+24L\\ mult.&\ 16N+32L \end{aligned}$$

The coefficients in the estimations for NR$^{\text{NV}}$ are large because complex voltages (E) and their conjugates (W) are independent variables in (16) and (17). The estimation in [6] does not consider this characteristic.

$(\mathbf{F}, \overline{\mathbf{F}})$ *in NR*$^{\text{WC}}$ *steps* (24):

$$\begin{aligned} load&\ 21N-9-5N_{PQ}+16L\\ store&\ 13N-7-3N_{PQ}+8L\\ add.&\ 8N-2-2N_{PQ}+8L\\ mult.&\ 10N-2-2N_{PQ}+8L \end{aligned}$$

$\mathbf{J}^{W}$ *in NR*$^{\text{WC}}$ *steps* (26):

$$\begin{aligned} load&\ 28N-20-12N_{PQ}+24L+8L_{PQ,PQ}+12L_{PQ,PV}+16L_{PV,PV}\\ store&\ 16N-12-4N_{PQ}+12L+8L_{PQ,PQ}+12L_{PQ,PV}+16L_{PV,PV}\\ add.&\ 12N-8-8N_{PQ}+12L\\ mult.&\ 8N+16L \end{aligned}$$

$(\Re(\mathbf{F}), \Im(\mathbf{F}))$ *in NR*$^{\text{WR}}$ *steps* (36):

$$\begin{aligned} load&\ 19N-7-5N_{PQ}+16L\\ store&\ 11N-5-3N_{PQ}+8L\\ add.&\ 8N-2-2N_{PQ}+8L\\ mult.&\ 10N-2-2N_{PQ}+8L \end{aligned}$$

$\mathbf{J}^{W\mathbb{R}}$ *in NR*$^{\text{WC}}$ *steps* (33):

$$\begin{aligned} load&\ 36N-28-12N_{PQ}+24L+20L_{PQ,PQ}+24L_{PQ,PV}+28L_{PV,PV}\\ store&\ 20N-16-4N_{PQ}+12L+20L_{PQ,PQ}+20L_{PQ,PV}+20L_{PV,PV}\\ add.&\ 16N-12-8N_{PQ}+12L+4L_{PQ,PV}+8L_{PV,PV}\\ mult.&\ 8N+16L \end{aligned}$$

$(\Re(\mathbf{F}), \Im(\mathbf{F}_{PQ})) - \mathbf{J}_2\mathbf{D}_1^{-1}\Im(\mathbf{F}_{PV})$ *in NR*$_{red}^{\text{WR}}$ *steps* (44):

$$\begin{aligned} load&\ 24N-12-12N_{PQ}+16L+6L_{PQ,PV}+6L_{PV,PV}\\ store&\ 13N-7-7N_{PQ}+8L+4L_{PQ,PV}+4L_{PV,PV}\\ add.&\ 9N-3-3N_{PQ}+8L+2L_{PQ,PV}+2L_{PV,PV}\\ mult.&\ 12N-4-4N_{PQ}+8L+2L_{PQ,PV}+2L_{PV,PV} \end{aligned}$$

$\mathbf{J}_{red}^{W\mathbb{R}}$ *in NR*$_{red}^{\text{WR}}$ *steps* (45):

$$\begin{aligned} load&\ 42N-34-18N_{PQ}+24L+20L_{PQ,PQ}+28L_{PQ,PV}+32L_{PV,PV}\\ store&\ 23N-19-7N_{PQ}+12L+20L_{PQ,PQ}+22L_{PQ,PV}+22L_{PV,PV}\\ add.&\ 17N-13-9N_{PQ}+12L+6L_{PQ,PV}+10L_{PV,PV}\\ mult.&\ 10N-2-2N_{PQ}+16L+2L_{PQ,PV}+2L_{PV,PV} \end{aligned}$$

Table I
THEORETICAL ESTIMATIONS OF THE LOADS REQUIRED FOR $\mathbf{F}$ AND $\mathbf{J}$ AT EACH STEP OF EACH STRATEGY

case	load	$\mathrm{NR}^{\mathrm{PC}}$	$\mathrm{NR}^{\mathrm{RC}}$	$\mathrm{NR}^{\mathrm{NV}}$	$\mathrm{NR}^{\mathrm{W}\mathbb{C}}$	$\mathrm{NR}^{\mathrm{W}\mathbb{R}}$	$\mathrm{NR}_{red}^{\mathrm{W}\mathbb{R}}$
1354peg.	**F**	53.3k	52.1k	103k	54.8k	52.1k	54.6k
	J	101k	136k	143k	88.9k	120k	124k
1888rte	**F**	70.4k	68.3k	136k	72.1k	68.3k	68.1k
	J	136k	180k	186k	114k	157k	159k
2000tex	**F**	80.5k	78.2k	156k	82.2k	78.2k	77.8k
	J	156k	206k	216k	130k	178k	181k
2383wp	**F**	84.1k	81.3k	162k	86.1k	81.3k	84.1k
	J	160k	214k	221k	138k	192k	198k
2746wp	**F**	96.0k	92.7k	184k	98.2k	92.7k	95.3k
	J	183k	244k	251k	157k	218k	224k
2868rte	**F**	106k	103k	205k	109k	103k	103k
	J	205k	271k	281k	172k	236k	241k
2869peg.	**F**	119k	116k	231k	122k	116k	121k
	J	229k	305k	323k	199k	270k	277k
3375wp	**F**	120k	116k	230k	123k	116k	118k
	J	230k	306k	315k	195k	271k	277k
6470rte	**F**	247k	237k	472k	250k	237k	231k
	J	480k	631k	654k	392k	541k	546k
9241peg.	**F**	403k	393k	782k	412k	393k	408k
	J	786k	1.05M	1.11M	682k	927k	951k
13659peg.	**F**	542k	539k	1.07M	566k	539k	565k
	J	1.05M	1.40M	1.48M	925k	1.26M	1.30M

Since loads are the most numerous and onerous operations [17], their actual amounts have been evaluated for the considered case studies and collected in Table I.

It is important to observe that, in every case, the construction of $\mathbf{F}$ requires about the same amount of loads in all strategies except for $\mathrm{NR}^{\mathrm{NV}}$, where it is almost double with respect to the others. For $\mathbf{J}$, $\mathrm{NR}^{\mathrm{W}\mathbb{C}}$ requires reduced quantities of loads with respect to all the other strategies, followed by $\mathrm{NR}^{\mathrm{PC}}$. $\mathrm{NR}^{\mathrm{W}\mathbb{R}}$ obtains the same matrices of $\mathrm{NR}^{\mathrm{RC}}$ with less loads, while $\mathrm{NR}_{red}^{\mathrm{W}\mathbb{R}}$ lies between them. Finally, $\mathrm{NR}^{\mathrm{NV}}$ is the most load requiring strategy.

2) Linear System Solution: the second comparison study consists in counting the amount of *flops* (floating point operations) required by the linear solver of MATLAB to solve (4) in each step of each strategy.

To this purpose, each case study is solved through all the considered strategies, starting from the initial guess given in the MATPOWER file. The stop criteria has been set as the reaching of 100 iterations and, at each step, the flops needed to solve the linear system are collected. The mean of the required flops has been calculated and collected in Table II.

Since all the introduced Jacobians are sparse matrices, MATLAB solves the associated linear systems with the direct solver of UMFPACK [18]. An estimate of the number of symbolic, numeric and solve flops is obtained by setting the debugging information of UMFPACK with the command `spparms('spumoni',2)`.

In all the cases, strategies with complex Jacobians ($\mathrm{NR}^{\mathrm{NV}}$, $\mathrm{NR}^{\mathrm{W}\mathbb{C}}$) require more flops for solving the linear system than the real-based ones ($\mathrm{NR}^{\mathrm{PC}}$, $\mathrm{NR}^{\mathrm{RC}}$, $\mathrm{NR}^{\mathrm{W}\mathbb{R}}$, $\mathrm{NR}_{red}^{\mathrm{W}\mathbb{R}}$). This difference is due to heavier complex operators compared to real operators.

Among complex-based strategies, $\mathrm{NR}^{\mathrm{W}\mathbb{C}}$ requires generally an increased number of flops with respect to $\mathrm{NR}^{\mathrm{NV}}$, since the sparsity of $\mathbf{J}^{w}$ in (26) is higher than that of $\mathbf{J}$ in (18).

Table II
MEANS OF THE FLOPS REQUIRED BY THE LINEAR SOLVER AT EACH STEP OF EACH STRATEGY.

case	$\mathrm{NR}^{\mathrm{PC}}$	$\mathrm{NR}^{\mathrm{RC}}$	$\mathrm{NR}^{\mathrm{NV}}$	$\mathrm{NR}^{\mathrm{W}\mathbb{C}}$	$\mathrm{NR}^{\mathrm{W}\mathbb{R}}$	$\mathrm{NR}_{red}^{\mathrm{W}\mathbb{R}}$
1354peg.	387k	516k	2.45M	2.90M	487k	603k
1888rte	783k	702k	3.74M	4.32M	711k	1.08M
2000tex	1.59M	1.68M	28.1M	28.2M	1.67M	2.82M
2383wp	835k	1.36M	12.6M	14.1M	1.36M	1.65M
2746wp	976k	1.41M	17.3M	12.2M	1.41M	1.88M
2868rte	1.22M	1.25M	5.71M	6.23M	1.20M	1.89M
2869peg.	1.05M	1.39M	6.41M	7.19M	1.42M	1.81M
3375wp	1.39M	1.98M	16.5M	20.9M	1.92M	2.75M
6470rte	3.01M	4.02M	25.6M	30.3M	4.04M	6.33M
9241peg.	5.90M	6.89M	39.9M	54.1M	6.87M	10.2M
13659peg.	8.04M	8.82M	50.8M	52.1M	8.82M	13.0M

As for the strategies with real Jacobians, $\mathrm{NR}^{\mathrm{PC}}$ has the lowest required flops, followed by $\mathrm{NR}^{\mathrm{RC}}$ and $\mathrm{NR}^{\mathrm{W}\mathbb{R}}$ (these last solve the same linear system). Despite the Jacobians of $\mathrm{NR}^{\mathrm{PC}}$ and $\mathrm{NR}_{red}^{\mathrm{W}\mathbb{R}}$ have the same size and sparsity, $\mathrm{NR}_{red}^{\mathrm{W}\mathbb{R}}$ is the worst among the real-based strategies. This because the linear system of $\mathrm{NR}_{red}^{\mathrm{W}\mathbb{R}}$ is solved through the *unsymmetric* technique of UMFPACK, while in all the other strategies the *symmetric* technique is used.

3) Time Quantification: to quantify the elapsed times for the adopted case studies, the implementations in MATLAB of the strategies are executed in an environment characterized by an AMD(R) Opteron 6176 SE processor with fixed 2.3 GHz CPU, 12MB cache and 32GB RAM, equipped with an up to date GNU/Linux Operating System.

Since MATLAB is an interpreted language, the times can be worse than those of a compiled language. Nevertheless, linear algebra is multi-threaded by default in MATLAB and this feature is fully exploited in the adopted environment, so that the obtained times are anyhow competitive.

Distinct time values for the equations and Jacobian construction and for the linear system solution are calculated with the MATLAB functions `tic` and `toc` in the respective code sections. As for the flops count, each case study is solved with the reaching of 100 iterations as stop criterion, resulting in data sets of 100 measures for each time value. Table III shows the minimum of each set, since it is the value less influenced by non-related processes.

In each case, the results related to the construction of $\mathbf{F}$ confirm the theoretical estimations discussed in Section V-A1: all strategies require comparable times, except for $\mathrm{NR}^{\mathrm{NV}}$ that doubles the time.

The times for the evaluation of $\mathbf{J}$, instead, show some differences with respect to the estimations in Section V-A1. In particular, there are two main variations: first, $\mathrm{NR}^{\mathrm{NV}}$ is faster than expected, so that instead of being the worst strategy, it is the second best after $\mathrm{NR}^{\mathrm{W}\mathbb{C}}$; second, $\mathrm{NR}_{red}^{\mathrm{W}\mathbb{R}}$ is the slowest strategy, while theoretically it should have been better than $\mathrm{NR}^{\mathrm{RC}}$ and $\mathrm{NR}^{\mathrm{NV}}$. These differences are caused by the well-optimized matrix operations in MATLAB: $\mathrm{NR}^{\mathrm{NV}}$ requires more calculations, but they can be collected in only four matrix products; on the contrary, the process described in Section IV leading to $\mathrm{NR}_{red}^{\mathrm{W}\mathbb{R}}$ requires an increased number of matrix products with respect to all the other strategies.

It is noteworthy that, despite they share the same results,

Table III
ELAPSED TIME IN *ms* FOR EVALUATING $\mathbf{F}$, $\mathbf{J}$ AND SOLVING THE LINEAR SYSTEM (*sol*) AT EACH STEP (MINIMUM VALUE OUT OF 100 ITERATIONS)

case	*ms*	NR^{PC}	NR^{RC}	NR^{NV}	$\text{NR}^{\text{W}\mathbb{C}}$	$\text{NR}^{\text{W}\mathbb{R}}$	$\text{NR}^{\text{W}\mathbb{R}}_{red}$
1354peg.	**F**	0.25	0.20	0.44	0.23	0.24	0.25
	J	1.33	1.90	1.35	1.00	1.76	2.42
	sol	13.82	15.97	19.58	20.68	16.25	15.48
1888rte	**F**	0.30	0.29	0.52	0.33	0.30	0.32
	J	1.75	2.20	1.68	1.20	2.15	3.20
	sol	17.61	18.73	27.05	29.45	18.73	23.11
2000tex	**F**	0.33	0.32	0.54	0.38	0.30	0.34
	J	1.84	2.53	1.80	1.32	2.35	3.34
	sol	24.47	26.92	57.02	61.96	27.49	32.74
2383wp	**F**	0.42	0.36	0.68	0.40	0.38	0.38
	J	2.18	2.94	2.15	1.56	2.75	4.29
	sol	26.60	33.01	48.66	51.41	32.83	33.56
2746wp	**F**	0.50	0.44	0.72	0.43	0.43	0.49
	J	2.55	3.42	2.40	1.73	3.21	4.63
	sol	26.93	34.89	61.03	51.34	32.80	36.36
2868rte	**F**	0.44	0.44	0.74	0.48	0.45	0.50
	J	2.67	3.26	2.52	1.81	3.17	4.78
	sol	31.64	29.13	41.54	45.26	28.23	34.53
2869peg.	**F**	0.59	0.47	0.81	0.49	0.41	0.57
	J	2.97	4.05	2.81	2.07	3.70	5.38
	sol	33.77	36.78	48.35	50.38	37.74	40.38
3375wp	**F**	0.60	0.50	0.85	0.51	0.49	0.57
	J	3.25	4.12	2.91	2.11	3.78	5.60
	sol	40.99	44.83	69.84	74.48	44.69	44.50
6470rte	**F**	1.13	0.93	1.59	0.91	0.99	1.09
	J	6.69	8.07	6.01	4.11	7.31	11.02
	sol	86.51	94.86	117.52	122.87	87.90	94.44
9241peg.	**F**	1.54	1.39	2.62	1.43	1.41	1.74
	J	10.88	15.98	10.50	7.33	12.63	18.86
	sol	136.65	156.40	191.70	210.77	157.60	165.84
13659peg.	**F**	2.03	1.86	3.60	2.08	1.95	2.23
	J	15.48	22.57	15.27	10.33	18.05	27.00
	sol	185.66	213.61	261.80	273.05	225.92	213.63

the construction of the Jacobian (13) in NR^{RC} is slower than that of the Jacobian (33) in $\text{NR}^{\text{W}\mathbb{R}}$.

For the solving time, as seen in V-A2, the real-based strategies are the better ones and, in particular, NR^{PC} is the fastest, followed by NR^{RC} and $\text{NR}^{\text{W}\mathbb{R}}$ (these last require almost the same time) and finally by $\text{NR}^{\text{W}\mathbb{R}}_{red}$ (that is disadvantaged by the UMFPACK *unsymmetric* solution technique). The strategies that involve complex systems (NR^{NV} and $\text{NR}^{\text{W}\mathbb{C}}$) respect exactly the estimations given by the number of required flops.

A major outcome from the above conducted experimental analysis is that the solving time accounts for most of the elapsed time, being one order of magnitude bigger than the other times. Then, NR^{PC} is the fastest strategy, followed by $\text{NR}^{\text{W}\mathbb{R}}$, NR^{RC}, $\text{NR}^{\text{W}\mathbb{R}}_{red}$ and finally by the complex ones.

However, it is pointed out that experimental results are strongly dependent on both the specific software implementation adopted (e.g., programming language, linked libraries, code optimization) and on its execution environment (computer architecture, such as threads and array processors [17] on multi-core or SIMD on many-core). Therefore, these aspects need to be taken into account when making the choice of the most appropriate strategy to employ.

In this respect, the value of conducting an analysis both on a theoretical basis and on a specific implementation setting is expected to be helpful from several perspectives. Among these, it could stimulate the development or more efficient implementations of theoretically promising strategies, targeting appropriate supporting technologies.

For example, investigating the adoption of many-core architectures, e.g., GPUs, looks a promising direction towards significantly reducing the linear system solution time so that strategies winning on reduced memory accesses (such as $\text{NR}^{\text{W}\mathbb{C}}$) could raise their competitiveness.

There exists a vast literature regarding the implementation of direct methods for sparse linear system solution that exploit both the host CPU and GPUs, such as the recent QR factorization presented in [19], and iterative methods, where the sparse matrix times vector subroutine is accelerated on GPUs [20].

At the moment, the MATLAB Parallel Computing Toolbox does not allow to accelerate on GPUs direct methods for sparse matrices and the fine tuning needed for the available iterative methods (i.e., `gmres` and `bcg`) is left for future work.

B. Convergence rate

The ability of each strategy to achieve convergence is analyzed examining their behavior in solving the adopted cases, with randomly changed initial parameters according to three different scenarios: 1) random initial voltages, 2) random level of loads and 3) random R/X ratio.

In particular, each strategy is tested with 20 maximum iterations and tolerance 10^{-10} on 10 sets of 100 random initial states, generated through normal distributions with changing standard deviation σ and mean depending on the scenario.

Since Jacobians of NR^{RC}, $\text{NR}^{\text{W}\mathbb{C}}$ and $\text{NR}^{\text{W}\mathbb{R}}$ are similar matrices, the convergence rates of these strategies are always equal. Similarly, the linear system in $\text{NR}^{\text{W}\mathbb{R}}_{red}$ is equivalent to that of $\text{NR}^{\text{W}\mathbb{R}}$. Thus, only data concerning NR^{RC} are shown.

For each value of σ in the considered ranges, the number of converged runs and of required steps to convergence, and information about the singular values of the Jacobian are collected to gain insights about convergence behaviors [21].

The singular values s of $\mathbf{J}$ correspond to the square root of the eigenvalues of $\overline{\mathbf{J}^t}\mathbf{J}$ and can be computed in a numerically stable way within MATLAB (through `svds`). As $\min(s)$ approaches 0 while $\max(s)$ increases, the conditioning number of $\mathbf{J}$ grows, producing an unreliable solution $\Delta\mathbf{X}$ of Equation (4) in NR. In addition, if many singular values of $\mathbf{J}$ are close to zero, then the correction $\Delta\mathbf{X}$ lies in a vector space with many almost parallel basis vectors. This implies that a small error in the computations can change considerably $\Delta\mathbf{X}$, so that the convergence of NR can go along an erratic path. Thus, the number of singular values that are smaller than a fixed threshold, i.e., $\#s < 0.01$ in the considered scenarios, represents a qualitative measure of the convergence behavior.

1) Initial Voltages: in the first convergence study, the initial voltages are randomly generated through a normal distribution with mean the voltages of the standard initial guess given in the MATPOWER file and variable σ.

In Fig. 1, on the left side, the convergence behavior for case6470rte is depicted and NR^{PC} is clearly worse than the other strategies. On the right side, in non-converged runs, the Jacobian of NR^{PC} has on average a greater number of small singular values and a bigger maximum singular value with respect to the other strategies. This behavior, characterizing

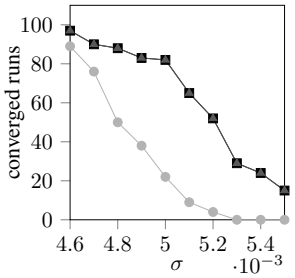

	$\min(s)$	$\#s<0.01$	$\max(s)$
NR^{PC}	$3.78e{-}05$	9.63	$1.32e{+}12$
NR^{RC}	$1.80e{-}03$	0.98	$3.86e{+}06$
NR^{NV}	$1.71e{-}03$	0.98	$1.24e{+}06$

Fig. 1. Convergence behavior for case6470rte [16] with random initial voltages: the effect of changing σ on the number of converged runs (on the left) and the mean of data concerning singular values of the Jacobian when the strategies do not converge (on the right).

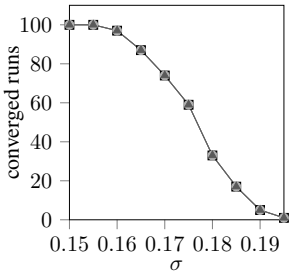

	$\min(s)$	$\#s<0.01$	$\max(s)$
NR^{PC}	$2.41e{-}03$	6.27	$1.20e{+}12$
NR^{RC}	$1.01e{-}02$	0.67	$1.56e{+}07$
NR^{NV}	$4.10e{-}03$	1.04	$1.66e{+}05$

Fig. 2. Convergence behavior for case2869pegase [16] with random level of loads: the effect of changing σ on the number of converged runs (on the left) and the mean of data concerning singular values of the Jacobian when the strategies do not converge (on the right).

Table IV
TOTAL NUMBER OF CONVERGED RUNS AND MEAN OF REQUIRED STEPS TO CONVERGENCE WITH DIFFERENT INITIAL VOLTAGES

case	σ		NR^{PC}	NR^{NV}	NR^{RC}
1354peg.	0.012-0.030	#conv	371	661	661
		#steps	7.12	9.70	9.70
1888rte	0.0048-0.0066	#conv	618	588	588
		#steps	8.47	14.92	14.92
2000tex	0.046-0.064	#conv	132	484	484
		#steps	7.97	11.51	11.51
2383wp	0.009-0.018	#conv	208	372	365
		#steps	7.98	11.95	11.95
2746wp	0.009-0.018	#conv	476	572	572
		#steps	7.48	8.65	8.65
2868rte	0.0036-0.0054	#conv	114	750	748
		#steps	8.36	13.95	13.94
2869peg.	0.014-0.023	#conv	287	556	556
		#steps	7.95	10.95	10.95
3375wp	0.005-0.014	#conv	422	656	656
		#steps	7.57	10.17	10.17
6470rte	0.0046-0.0055	#conv	288	625	625
		#steps	8.15	17.52	17.52
9241peg.	0.0050-0.0068	#conv	418	550	550
		#steps	8.30	8.97	8.97
13659peg.	0.0030-0.0057	#conv	711	519	519
		#steps	7.45	13.99	13.99

Table V
TOTAL NUMBER OF CONVERGED RUNS AND MEAN OF REQUIRED STEPS TO CONVERGENCE WITH DIFFERENT LEVELS OF LOADS

case	σ		NR^{PC}	NR^{NV}	NR^{RC}
1354peg.	0.25-0.43	#conv	755	755	755
		#steps	5.77	7.52	7.52
1888rte	0.0070-0.0088	#conv	565	565	565
		#steps	6.28	6.74	6.74
2000tex	0.150-0.177	#conv	529	529	529
		#steps	6.74	7.62	7.62
2383wp	0.400-0.445	#conv	670	670	670
		#steps	8.24	10.62	10.62
2746wp	0.51-0.60	#conv	596	596	596
		#steps	6.87	7.45	7.45
2868rte	0.0048-0.0057	#conv	677	677	677
		#steps	6.77	7.39	7.39
2869peg.	0.150-0.195	#conv	573	573	573
		#steps	7.13	9.76	9.76
3375wp	0.180-0.225	#conv	456	456	456
		#steps	6.33	7.30	7.24
6470rte	0.0050-0.0068	#conv	656	656	656
		#steps	5.73	6.45	6.45
9241peg.	0.090-0.099	#conv	683	683	683
		#steps	7.30	11.29	11.29
13659peg.	0.001-0.004	#conv	200	200	200
		#steps	6.50	7.32	7.32

most of the NR^{PC} non-converged runs, implies that NR^{PC} is more prone to follow erratic paths. The non-convergence of the other strategies can instead be linked to an oscillating behavior since the average $\#s < 0.01$ is small and the mean of $\max(s)$ remains close to 10^6 (an expected order of magnitude for $\max(s)$ of Jacobians related to transmission grids).

In Table IV, the total number of converged runs over the 1000 considered and the mean of the number of required steps to converge are shown. Except for case13659pegase, NR^{PC} is in general the strategy that converges in a lower number of cases, while the other strategies have similar behaviors. Notice that, when NR^{PC} converges, it requires less steps than the other strategies.

2) Level of Loads : instead of studying the strategies behavior with generic level of loads, the more unstable scenario of overloaded network is considered. Thus, active and reactive powers (P and Q) are increased multiplying them by a random factor generated through the absolute value of a normal distribution with mean 1 and variable σ.

The common behavior of convergence is well represented in Fig. 2, where the collected data for case2869pegase are represented: on the left side it is shown that all the strategies converge in the same number of runs; the right side indicates that, as for the previous scenario, the singular values of the Jacobians in non-converged situations lead NR^{PC} to an erratic path and the other strategies to an oscillating behavior.

In Table V is clear that, in each case study, the total number of converged runs is the same for all strategies and the average number of steps required to convergence is reduced for NR^{PC} with respect to the other strategies.

3) R/X Ratio : finally, random R and X for each line are obtained, so that different values of the R/X ratio are tested. The random initial situations are generated with mean the values R and X of the MATPOWER file and variable σ.

As seen on the left of Fig. 3, related to case2383wp, generally NR^{PC} converges less than the other strategies. As in the previous scenarios, from the right side of Fig. 3, the behavior of non-converged runs is generally erratic for NR^{PC} and oscillatory for the other strategies.

In Table VI is shown that NR^{PC} converges in a slightly minor number of runs and, again, requires generally less steps to reach convergence with respect to the other strategies.

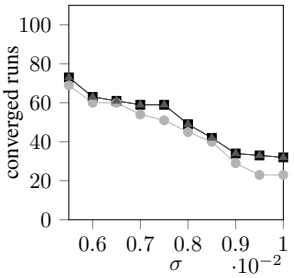

	min(s)	#s<0.01	max(s)
NR^{PC}	6.97e−03	7.21	3.93e+13
NR^{RC}	2.70e−02	0.21	6.11e+06
NR^{NV}	2.57e−03	1.65	6.23e+05

Fig. 3. Convergence behavior for case2383wp [16] with random R/X ratio: the effect of changing σ on the number of converged runs (on the left) and the mean of data concerning singular values of the Jacobian when the strategies do not converge (on the right).

Table VI
TOTAL NUMBER OF CONVERGED RUNS AND MEAN OF REQUIRED STEPS TO CONVERGENCE WITH DIFFERENT R/X RATIOS

case	σ		NR^{PC}	NR^{NV}	NR^{RC}
1354peg.	0.0001-0.0019	#conv	577	586	586
		#steps	4.82	5.09	5.10
1888rte	0.0020-0.0065	#conv	392	399	399
		#steps	5.60	6.87	6.87
2000tex	0.001-0.010	#conv	479	497	497
		#steps	4.45	4.98	4.98
2383wp	0.0055-0.0100	#conv	454	504	505
		#steps	6.47	8.23	8.23
2746wp	0.0005-0.0095	#conv	626	642	642
		#steps	5.34	5.97	5.97
2868rte	0.0015-0.0060	#conv	413	432	432
		#steps	5.66	7.45	7.45
2869peg.	0.0001-0.0019	#conv	494	519	519
		#steps	6.97	6.37	6.39
3375wp	0.0005-0.0050	#conv	604	619	619
		#steps	4.84	5.05	5.08
6470rte	0.0010-0.0055	#conv	478	483	483
		#steps	5.19	6.38	6.39
9241peg.	0.0001-0.0010	#conv	540	548	547
		#steps	7.00	6.35	6.35
13659peg.	0.0005-0.0050	#conv	459	451	451
		#steps	6.41	8.19	8.19

VI. CONCLUSIONS AND FUTURE WORK

When solving the PFEs by using NR, strategies based on real or complex variables have been studied, so to address the different performances to satisfy varying requirements dictated by diverse usage contexts.

First, this paper explored the application of Wirtinger calculus to the complex formulation of the PFEs. The resulting strategy ($NR^{W\mathbb{C}}$) is already present in the literature. However, the novel development highlights the centrohermitian structure of the Wirtinger Jacobian, then exploited to obtain an equivalent strategy ($NR^{W\mathbb{R}}$), which turns out to be a more efficient variant of the classical formulation with rectangular coordinates (NR^{RC}). A reduced real-based strategy is also proposed, trying to further improve the obtained ones.

Second, a detailed comparison among existing and new proposed strategies has been conducted, in terms of computational efforts and convergence rates. Some important aspects are emphasized. Regarding computational costs of the linear system construction, $NR^{W\mathbb{C}}$ is the best and $NR^{W\mathbb{R}}$ is faster than the equivalent NR^{RC}. For the linear system solution, the classical formulation with polar coordinates (NR^{PC}) is the fastest. Moreover, NR^{PC} converges in less runs than the others; however, when it does, it requires less steps than the others.

In conclusion, besides exploring the application of Wirtinger calculus with some interesting results, strengths and weaknesses of the addressed strategies have been investigated, in order to help the choice of the approach to employ to solve power-flow equations for a specific power system under study.

Extensions are foreseen in several directions, including:

- to further analyze the matrices properties in the considered strategies in order to improve their performance;
- to explore the behavior of parallel implementations;
- to investigate applications of Wirtinger calculus in other electric contexts, such as the Optimal Power Flow.

REFERENCES

[1] J. J. Grainger and W. D. J. Stevenson, *Power system analysis*. McGraw-Hill, Inc., 1994.

[2] W. F. Tinney and C. E. Hart, "Power flow solution by Newton's method," *IEEE Trans. on Power App. and Syst.*, no. 11, pp. 1449–1460, 1967.

[3] A. Gomez-Exposito, A. Conejo, and C. Canizares, *Electric Energy Systems: Analysis and Operation*, ser. Electric Power Engineering Series. CRC Press, 2017.

[4] R. D. Zimmerman, C. E. Murillo-Sanchez, and R. J. Thomas, "MATPOWER: Steady-state operations, planning, and analysis tools for power systems research and education," *IEEE Trans. on Power Syst.*, vol. 26, no. 1, pp. 12–19, 2011.

[5] H. Le Nguyen, "Newton-raphson method in complex form," *IEEE Trans. on Power Syst.*, vol. 12, no. 3, pp. 591 – 595, 1997.

[6] T. T. Nguyen and C. T. Vu, "Complex-variable Newton-Raphson load-flow analysis with FACTS devices," in *2005/2006 IEEE/PES Transmission and Distribution Conference and Exhibition*, 2006, pp. 183–190.

[7] J.-M. Muller, *Elementary Functions. Algorithms and Implementation*. Springer, 2006.

[8] J. E. Tate and T. J. Overbye, "A comparison of the optimal multiplier in polar and rectangular coordinates," *IEEE Trans. on Power Syst.*, vol. 20, no. 4, pp. 1667–1674, 2005.

[9] V. Quintana and N. Müller, "Studies of load flow methods in polar and rectangular coordinates," *Electric Power Systems Research*, vol. 20, no. 3, pp. 225 – 235, 1991.

[10] W. Wirtinger, "Zur formalen theorie der funktionen von mehr komplexen veränderlichen," *Mathematische Annalen*, vol. 97, no. 1, pp. 357–375, 1927.

[11] Z. Wang, B. Cui, and J. Wang, "A necessary condition for power flow insolvability in power distribution systems with distributed generators," *IEEE Trans. on Power Syst.*, vol. 32, no. 2, pp. 1440–1450, 2017.

[12] J. Bandler, M. El-Kady, and H. Gupta, "Practical complex solution of power flow equations," *IEEE Trans. on Circuits and Syst.*, vol. 29, no. 11, pp. 772–775, 1982.

[13] F. J. Gonzalez-Vazquez, "The differentiation of functions of conjugate complex variables: application to power network analysis," *IEEE Trans. on Educ.*, vol. 31, no. 4, pp. 286–291, 1988.

[14] A. Lee, "Centrohermitian and skew-centrohermitian matrices," *Linear Algebra Appl.*, vol. 29, Suppl. C, pp. 205–210, 1980.

[15] MathWorks, *MATLAB R2018a*, The Mathworks, Inc., Natick, Massachusetts, 2018.

[16] R. D. Zimmerman, C. E. Murillo-Sanchez *et al.*, *MATPOWER: A MATLAB Power System Simulation Package*, version 6.0.

[17] J. P. Hulskamp, S. Chan, and J. F. Fazio, "Power flow outage studies using an array processor," *IEEE Trans. on Power and App. Syst.*, no. 1, pp. 254–261, 1982.

[18] T. A. Davis, "Algorithm 832: UMFPACK V4.3 - an unsymmetric-pattern multifrontal method," *ACM Trans. on Math. Softw.*, vol. 30, no. 2, pp. 196–199, 2004.

[19] S. N. Yeralan, T. A. Davis, W. M. Sid-Lakhdar, and S. Ranka, "Algorithm 980: Sparse QR factorization on the GPU," *ACM Trans. on Math. Softw.*, vol. 44, no. 2, pp. 17:1–17:29, 2017.

[20] N. Bell and M. Garland, "Efficient sparse matrix-vector multiplication on CUDA," NVIDIA, Tech. Rep., 2008.

[21] Y.-Q. Shen and T. J. Ypma, "Newton's method for singular nonlinear equations using approximate left and right nullspaces of the jacobian," *Applied Numerical Mathematics*, vol. 54, no. 2, pp. 256 – 265, 2005, 6th IMACS.